Mechanism of Auxin Interaction with Auxin Binding Protein (ABP1): A Molecular Dynamics Simulation Study

Branimir Bertoša,* Biserka Kojić-Prodić,* Rebecca C. Wade,† and Sanja Tomić*
*Ruđer Bošković Institute, Zagreb, Croatia; and †Molecular and Cellular Modeling Group, EML Research, Heidelberg, Germany

ABSTRACT Auxin Binding Protein 1 (ABP1) is ubiquitous in green plants. It binds the phytohormone auxin with high specificity and affinity, but its role in auxin-induced processes is unknown. To understand the proposed receptor function of ABP1 we carried out a detailed molecular modeling study. Molecular dynamics simulations showed that ABP1 can adopt two conformations differing primarily in the position of the C-terminus and that one of them is stabilized by auxin binding. This is in agreement with experimental evidence that auxin induces changes at the ABP1 C-terminus. Simulations of ligand egress from ABP1 revealed three main routes by which an auxin molecule can enter or leave the ABP1 binding site. Assuming the previously proposed orientation of ABP1 to plant cell membranes, one of the routes leads to the membrane and the other two to ABP1's aqueous surroundings. A network of hydrogen-bonded water molecules leading from the bulk water to the zinc-coordinated ligands in the ABP1 binding site was formed in all simulations. Water entrance into the zinc coordination sphere occurred simultaneously with auxin egress. These results suggest that the hydrogen-bonded water molecules may assist in protonation and deprotonation of auxin molecules and their egress from the ABP1 binding site.

INTRODUCTION

The multifunctional phytohormone and mobile signaling molecule, auxin (indole-3-acetic acid, IAA), controls almost every aspect of a plant's life (1–6). Auxin regulates essential processes of plant morphogenesis, organogenesis, and reproduction, such as elongation, secondary growth (thickening), branching (apical dominance), and tropic response (directed growth in response to external stimuli such as light and gravity) of stems and roots, the initiation and differentiation of vascular tissues, and the development of fruits and seeds (1,7). At the cellular level, auxin affects division, expansion, differentiation, and turgor (the pressure that the protoplast exerts on the cell wall from within). Some short-term effects may reflect direct auxin impact on cell membrane proteins; most other responses appear to include changes in gene expression (8). Thus, the acronym IAA for indole-3-acetic acid can also be an abbreviation for ''Influences Almost Anything'' as used by Weijers and Jürgens (9). In performing its versatile roles, auxin displays characteristics of a hormone although recent findings advocate in favor of its morphogenic function (10–12). Auxin has been found in all members of the plant kingdom, occurring in micromolar quantities or less. It can be present in a free form or as a conjugate covalently bound to sugars, peptides, amino acids, or proteins and is also available from indole-3-butyric acid (IBA). Its conjugates contribute to the regulation of free hormone levels in plant tissue (1–5).

The first recognition of auxin's activities was deduced from the growth responses of roots in 1872 (13) and stems in 1880 (14). The discovery of the first plant hormone, later termed ''auxin'' (originating from the Greek word *auxein* meaning ''to grow''), intrigued scientists to discover its chemical identity; Went (1927) (15,16), Kögel and Kostermans (1934) (17), and Thiemann (1935) (18) detected indole-3-acetic acid. Now, more chemically related molecules of this class, both natural and synthetic, acting as plant growth substances or as selective herbicides, are known. They are collectively termed ''auxins'' (1–6).

Plant growth is characterized by its adaptability to continuous changes of the environment. One key issue in a plant's adaptation are the processes of signaling which enable plants to react to environmental conditions, both normal (nutrients, light, oxygen, water, temperature, gravity, wind) and extreme (high temperatures, cold, pollutants, droughts, high salinity, pathogens). Thus, signal transduction in plants involves cross-talk with the environment. Plants have developed signaling mechanisms which are among the most complex in living organisms and remain a challenge for plant physiologists to decipher. Nevertheless, many aspects of plant growth have been found to depend on transport of auxin across tissues directed by specific transport proteins. The last few years have seen tremendous progress in the identification of the proteins responsible for auxin transport. Auxin efflux carriers (PINs) (12,19–22) have been found to act directly in transporting auxin out of the cells, probably independently of the activities of the PGP transmembrane protein family. The protein AUX1, an auxin influx carrier, has been found to mediate cellular influx of auxin (21). However, these findings are just the beginning of uncovering a complex signaling network (6,23).

Identification of auxin receptors involved in signaling systems is a particularly significant step toward understanding the molecular basis of auxin action, but also a complex

Submitted March 20, 2007, and accepted for publication July 27, 2007.

Address reprint requests to Sanja Tomić, Tel.: 351-1-5671-251; E-mail: sanja.tomic@irb.hr.

Editor: Ivet Bahar.

0006-3495/08/01/27/11 $2.00

doi: 10.1529/biophysj.107.109025

venture. The involvement of auxin in a diverse array of critical physiological functions may well be mediated by an equally diverse array of receptors and/or an intricate network of signaling cascades. Two auxin receptors are presently under consideration (24,25): Auxin Binding Protein 1 (ABP1), with a known three-dimensional molecular structure (26) but an incompletely known physiological role (1,2,10,11,25), and a transport inhibitor response protein (TIR1) that is structurally not characterized but has a role as the auxin receptor for auxin-mediated transcriptional regulation (27,28). TIR1 regulates the expression of specific auxin-responsive genes by stimulating the ubiquitinylation and subsequent degradation of Aux/IAA transcriptional repressor proteins. It does not appear to participate in auxin transport (24,27–29).

Auxin Binding Protein 1 (ABP1) is ubiquitous in green plants but its physiological role is not understood yet ((3) and references therein (6,23,30–32)). It was detected in 1977 ((3) and references therein), purified in 1985 ((3) and references therein), and in 2002, its crystal structure was solved (PDB codes 1LR5 and 1LRH) (26). ABP1 binds auxin at concentrations corresponding to physiological concentrations for auxin individual activities (3,33) with the optimal pH for binding being 5.0–6.0 (24). Several reports have suggested that ABP1 is involved in some cellular responses to auxin, such as cell elongation, cell division, plasma membrane hyperpolarization, and ion fluxes in protoplasts ((6) and references therein, (34–36)). According to these reports, ABP1 is located on the outer side of the plasma membrane, as would be expected for a hormone receptor. However, ABP1 contains a KDEL sequence at the C-terminus that identifies ABP1 as a protein that is targeted to the endoplasmic reticulum (ER). Indeed, ABP1 is predominantly situated in the ER (37–39) and only a small amount manages to escape from the ER to the plasma membrane. However, at the endoplasmic reticulum, the pH is too high for efficient auxin binding (23,40). Thus, ABP1 does not bind auxin within the ER even though this is the predominant subcellular location for this receptor.

Sequence analysis and the crystal structure indicate that ABP1 belongs to the cupin protein superfamily (26,41) characterized by the predominance of an anti-parallel β-sheet motif. Its structural similarity to manganese oxalate-oxidase, PDB code 1FI2 (acting as oxidoreductase) (42) and other enzymatic cupins, and the role of zinc in the active site of ABP1 raise the question of its possible enzymatic function (41). The crystallographic asymmetric unit consists of two ABP1 homodimers. To our knowledge, no cooperativity between subunits of the dimer has been reported, and the oligomeric state of ABP1 in vivo is unknown.

Before the ABP1 crystal structure was solved, QSAR analysis based solely on the structures of auxin and auxin-related molecules was possible. Different approaches were used to develop models (43–49) that related the biological activity of the compounds to their structural features. The models enabled identification of structural features important for auxin activity and classification of auxin-related compounds. The crystal structure of ABP1 (26) enables computational docking studies which can contribute to understanding of the ABP1 mechanism (43). Using different computational methods, the interactions of auxin-related molecules with ABP1 can be studied and hypotheses on the ABP1 function(s) proposed. Currently, there are only limited experimental data about ABP1 trafficking and its interactions with auxin to compare against computational results. A single report on the measurement of auxin binding to the purified ABP1 is available (50); only a few compounds were investigated and compounds with antiauxin activity or with auxin structural features but lacking auxin activity were not studied. In other cases, experimental data were collected using unpurified ABP1 (51), which contained other biological material that might affect auxin binding.

In this work, we used the crystal structures of ABP1 and ABP1 in complex with 1-naphtaleneacetic acid (NAA) (26) and performed a docking study for some auxin-related molecules. Molecular dynamics simulations were used to investigate changes in protein conformation and stability induced by docking compounds with differing auxin or antiauxin activity in the ABP1 binding site. In particular, the conformational variation in the C-terminus of ABP1 and its relation to auxin binding was investigated. Standard molecular dynamics simulations and the random acceleration molecular dynamics (RAMD) simulation method (52–54) were used to investigate possible routes for the transport of auxin compounds in and out of the ABP1 binding site. The relation of these routes to ABP1 receptor function was explored, as was the role of a hydrogen-bonded water network in auxin binding and unbinding.

METHODS

System preparation

The recently determined crystal structures of the unbound auxin-binding protein 1 (ABP1) and of its complex with 1-NAA were extracted from the Brookhaven Protein Databank (55) (codes 1LR5 and 1LRH, respectively). The crystal structures of the protein consist of four almost identical monomers (root mean-square deviation (RMSDs) between the different subunit backbones are from 0.24 to 0.57 Å). The C-termini of monomers A and D make intermolecular contacts and have lower mobility, as described by atomic temperature factors, whereas monomers B and C are not involved in contacts and their mobility is approximately twice as high. The structures of the free protein and the protein in the complex are very similar (RMSD of backbone atoms between the equivalent subunits ranges from 0.18 to 0.23 Å). For the molecular modeling study, we used subunits A and C and the 73 water molecules found in the crystal structure within 3 Å of the protein heavy atoms of the selected subunits. Although ABP1 is dimeric in solution and in the crystal ((26) and references therein), we used the monomeric form for the simulations since, to our knowledge, no cooperativity between subunits of the dimer have been reported. Complexes between ABP1 and the following auxin-related compounds were built: 1-naphtaleneacetic acid (NAA), indole-3-acetic acid (IAA), 4-chloro-indole-3-acetic acid (4-Cl-IAA), indole-3-isobutyric acid (IIBA), and benzoic acid (BA). The compounds were either manually docked into the ABP1 binding site, or the binding modes obtained from previous Monte Carlo searches (43) were used. Parameters for auxin-related compounds were derived using Antechamber in

the AMBER 8.0 program package (56,57). Zinc parameters from our previous calculations were used (58): $r = 1.22$ Å, $\varepsilon = 0.25$ kcal/mol, and charge $+2e$.

Polar hydrogen atoms were added using the WHATIF software (59), which adds hydrogens in positions to optimize the hydrogen-bond network in the protein. A few amino-acid residues were flipped by WHATIF to the other, energetically more favorable rotamer, namely His^{27}, Asn^{35}, Asn^{110}, His^{114}, and His^{140} in 1LR5-A, and His^{27}, His^{36}, Gln^{56}, Gln^{86}, and His^{140} in 1LRH-A. Nonpolar hydrogen atoms were added with Tleap, which is part of the AMBER 8 program package.

Simulations

The protein was placed in the center of a truncated octahedron that was filled with TIP3P type water molecules. Besides water molecules, Na^+ and Cl^- ions were added to neutralize the system and placed in the vicinity of charged amino acids at the protein surface. The resulting system of ~20,000 atoms was simulated using periodic boundary conditions and particle-mesh Ewald for calculation of electrostatic interactions. The AMBER ff03 (60) force field of Duan et al. was used.

Before molecular dynamics (MD) simulations, the protein geometry was optimized in three cycles with different constraints. In the first cycle, water molecules were relaxed, while the protein and substrate atoms were constrained using a harmonic potential with a force constant of 32 kcal/(mol × $Å^2$). In the second cycle, the same constraint was put on all nonhydrogen atoms of the protein and the substrate; the goal of this cycle was relaxation of hydrogen atoms. Finally, in the third cycle, only the position of the zinc was constrained as it was also constrained during the MD simulations. The energy minimization procedure was the same in all three cycles: 100 steps of steepest descent were followed by 400 steps of conjugate gradient optimization. The final gradient was ~0.1 kcal/(mol × Å).

After energy minimization, the system was equilibrated during 300 ps. For the first 100 ps of equilibration, the volume was constant. During the first 80 ps, the temperature was linearly increased from 0 to 300 K and during the remaining 20 ps it was held constant. In the next 200 ps of equilibration, temperature and pressure were held constant ($T = 300$ K, $P = 1$ atm). The goal of the equilibration was to achieve a stable system with constant density.

The equilibrated system was then subjected to a 5 ns molecular dynamics simulation at constant temperature and pressure (300 K, 1 atm). The temperature was held constant using Langevin dynamics with a collision frequency of 1 ps^{-1}: The time step was 1 fs and the SHAKE algorithm was not used. Structures were sampled every 0.1 ps over 5 ns.

Simulations with variations in temperature

For the ABP1 and its complexes with NAA, IAA, and IIBA, simulations were repeated using a procedure including temperature variations. After equilibration, MD simulations were run at 300 K for 100 ps, and then the temperature was linearly increased to 500 K during 100 ps. From 200 ps to 600 ps, the system was held at 500 K and finally, the temperature was linearly decreased to 300 K during the next 200 ps (Fig. 1). From 800 ps to 5 ns, the simulation was the same as previously described. The goal of the simulations with variation in temperature was to provoke possible conformational changes for which the 5-ns simulation at 300 K was too short.

The trajectories were visualized using the MD Display (61) and Chimera (62) software, and analyzed using the ptraj program from the AMBER 8 program package.

Simulations of auxin expulsion from the ABP1 active site

To explore possible pathways used by auxin-related molecules to enter and leave the ABP1 active site, random acceleration molecular dynamics (RAMD) simulations (52–54) were performed. To simulate an auxin egress from the ABP1 active site is very demanding because it might occur on a timescale much larger than the timescale currently possible for standard MD simulations of proteins. The RAMD method overcomes this problem by applying a small, artificial, randomly orientated force to the center of mass of the ligand to enhance the probability of its spontaneous exit. We have performed a series of RAMD simulations to 1), find the most appropriate parameterization of the force (acceleration from 0.1 to 0.25 kcal/(g × Å) with atomic mass in units of g/mol was used) considering the simulation timescale and the protein reorganization; and 2), to obtain statistically significant results. Different starting structures of ABP1 complexes with NAA and IAA were used. The RAMD simulations were run for 150 ps (in a few cases for 400 ps) or until the distance between the centers of mass of ABP1 and the auxin molecule became larger than 30 Å. The time step was the same as used in MD simulations (1 fs). The direction of the force was kept for 40 timesteps (40 fs). If during this period, a ligand did not move more than 0.01 Å, a new direction was chosen randomly, otherwise the same force was applied for the next 40-timestep period.

Tunnels for auxin entrance/exit were also explored with the CAVER software (63). It finds tunnels in a protein structure from a user-defined starting point to the exterior by placing a grid over the protein and connecting those points that have more empty space around. The grid spacing was set to 0.8 Å and the zinc ion was chosen as the starting point in the protein.

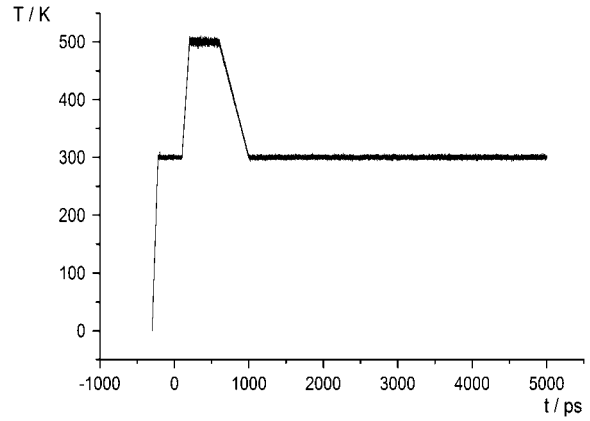

FIGURE 1 Temperature variation during equilibration (from −300 to 0 ps) and during the production run (from 0 to 5000 ps).

RESULTS AND DISCUSSION

MD Simulations at 300 K show a stable protein structure and reveal a network of hydrogen-bonded water molecules from the ABP1 binding site to the protein surface

In the crystal structure of ABP1 (26), the zinc ion is coordinated by three histidines (His^{57}, His^{59}, His^{106}), glutamate 63 and a water molecule. In the crystal structure of the ABP1 complex with NAA, a coordinated water molecule is replaced by bidentately coordinated 1-NAA (26) (Fig. 2). The conformations of the free protein and its NAA-complex do not reveal other significant differences, though this structural conservation might be a consequence of the crystal packing (26). Molecular dynamics (MD) simulations were used to monitor changes in the protein active site and protein conformation introduced by binding auxin and auxin-related compounds.

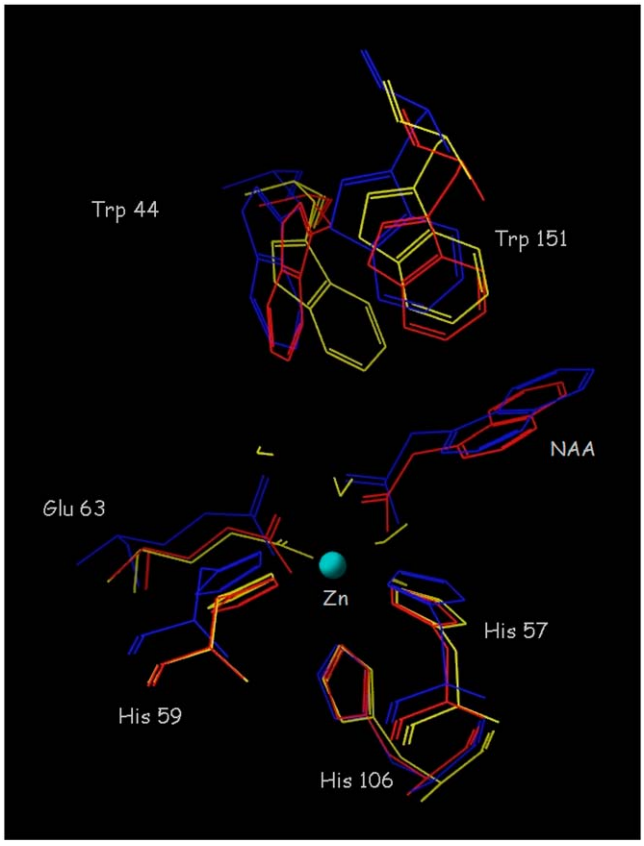

FIGURE 2 Comparison of the active site of ABP1 in the crystal structure of its complex with NAA (*blue*), the average structure from a 5 ns simulation of the ABP1-NAA complex (*red*), and the average structure from a 5 ns simulation of the free ABP1 (*yellow*).

During 5-ns simulations at a constant temperature of 300 K of ABP1 in its unbound state and of its complexes with NAA, IAA, 4-Cl-IAA, IIBA, and BA, no significant conformational changes were detected in the protein. The active site topology was almost the same in all simulations. In the literature (1,26,64), attention has been given to the role of tryptophan 151 in the auxin binding. Therefore, we monitored its dynamics during the simulations. In the crystal structure of ABP1 and during the 5-ns simulations, the aromatic ring planes of tryptophan 151 and the auxins were perpendicular (Fig. 2). The two aromatic rings participate in a π-π face-to-edge interaction.

The average RMSD of the protein backbone from the crystal structure was similar in simulations of unbound ABP1 (1.41 Å) and of the ABP1-NAA complex (1.48 Å). (The RMSD of the protein backbone between the starting structures for these two simulations is 0.51 Å.)

The zinc coordination is stable during the 5-ns simulations. In simulations of the free ABP1, glutamate 63 is initially bidentately coordinated to the Zn^{2+} ion but, after 960 ps of simulation, it moves away and coordinates the Zn^{2+} monodentately. The carboxyl oxygen of glutamate 63 that left the Zn coordination sphere spent most of the time at ~3 Å distance from the Zn^{2+} ion (Fig. 3), stabilized by hydrogen bonds with water molecules.

During all simulations, some water molecules from the bulk solvent (described using an explicit solvent model, see Methods) moved into the binding site through the channel running (through the loop Lys^{125}-Arg^{129}) from the protein surface to the active site (Fig. 4). The process was initiated in the early phases of all the simulations performed, often during the equilibration, resulting in a network of hydrogen-bonded water molecules that spanned from the active site to arginine 129 and lysine 125, amino acids located on the protein surface. Water molecules participating in the network replaced each other during the simulations, but the network was maintained until the end of the simulations. The water molecule located in the active site participates in hydrogen bonds to the carboxyl group of glutamate 63 and the carboxyl group of the auxin-related molecule (Fig. 4).

The fact that the hydrogen-bond network appeared in all simulations in approximately the same fashion clearly shows that water molecules in the active site can easily be exchanged with bulk water.

MD Simulations with variations in temperature show conformational changes at the C-terminus and Trp^{151} that are affected by binding of an auxin compound in the ABP1 binding site

Small differences in the protein structure that appeared at the end of the simulations of the free ABP1 and complexes of ABP1 with an auxin-related compound at room temperature encouraged us to perform a series of simulations in which the

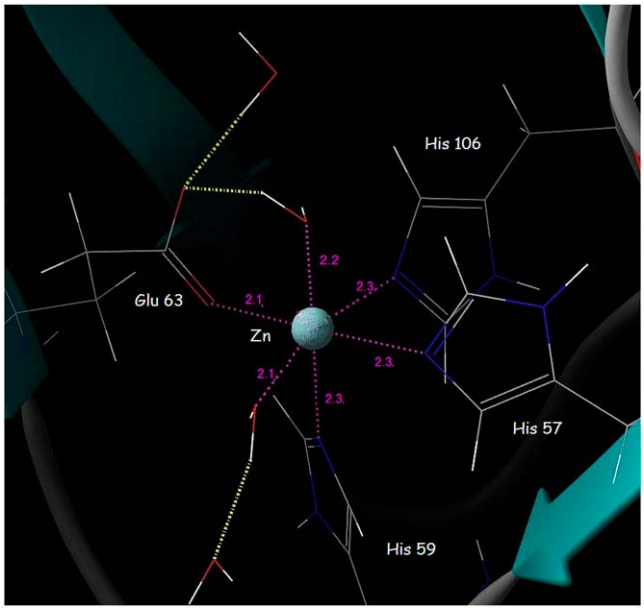

FIGURE 3 The octahedral coordination of the Zn^{2+} ion in the active site of the free ABP1 observed after 3.5 ns of MD simulations. The metal-ligand distances (Å) are in magenta.

FIGURE 4 The network of hydrogen-bonded water molecules spanning from the ABP1 binding site to the protein surface formed during the 5-ns MD simulation of the ABP1-IIBA complex. Hydrogen bonds are represented by dotted yellow lines. ABP1 is shown in cartoon representation with the backbone atoms of Lys^{125} and Arg^{129} and all atoms of Glu^{63}, His^{57}, His^{59}, and His^{106} in stick representation and the Zn ion represented by a sphere.

temperature was briefly increased above 300 K (see Methods). The goal of this kind of simulation was to give the system enough kinetic energy to overcome some energy barriers and to achieve conformational changes that might occur at room temperature but during a time period that is longer than our simulations. The temperature was linearly increased from room temperature to 500 K, kept constant for 400 ps, and then linearly decreased to 300 K (see Methods). These simulations were run for the free ABP1 and for ABP1 complexes with NAA, IAA, and 3-IIBA. The increase of kinetic energy of the system initiated the movement of flexible parts of the ABP1. Simulations under elevated temperatures of the free ABP1 and its complexes with auxin-related molecules revealed conformational changes. During the 400-ps interval of MD simulations of the free ABP1 (at 500 K), the conformation of the C-terminus was more extended compared to the conformation observed in the crystal structure, and tryptophan 151 was pulled out of the active site (Fig. 5 *A*). Simulations of the free ABP1 at elevated temperature were repeated a few times, revealing the conformational changes of the C-terminus. At the end of the simulation period at elevated temperature (see Methods), tryptophan 151 was completely out of the binding site and the C-terminus had a mostly extended α-helical conformation. This conformation seemed to be energetically stable at 300 K as the protein retained it after cooling the system down (Fig. 5 *A*). Energy minimization of the crystal structure and the structure obtained after 1.5 ns of the simulation with variation of temperature showed that the structure with the extended C-terminus is energetically more favorable (-7.84×10^6 cal/mol with gradient of 9.87×10^{-2} kcal/(mol $\times$ Å)) than the compact crystal structure (-7.36×10^6 cal/mol, gradient 9.59×10^{-2} kcal/(mol $\times$ Å)). It is possible that such

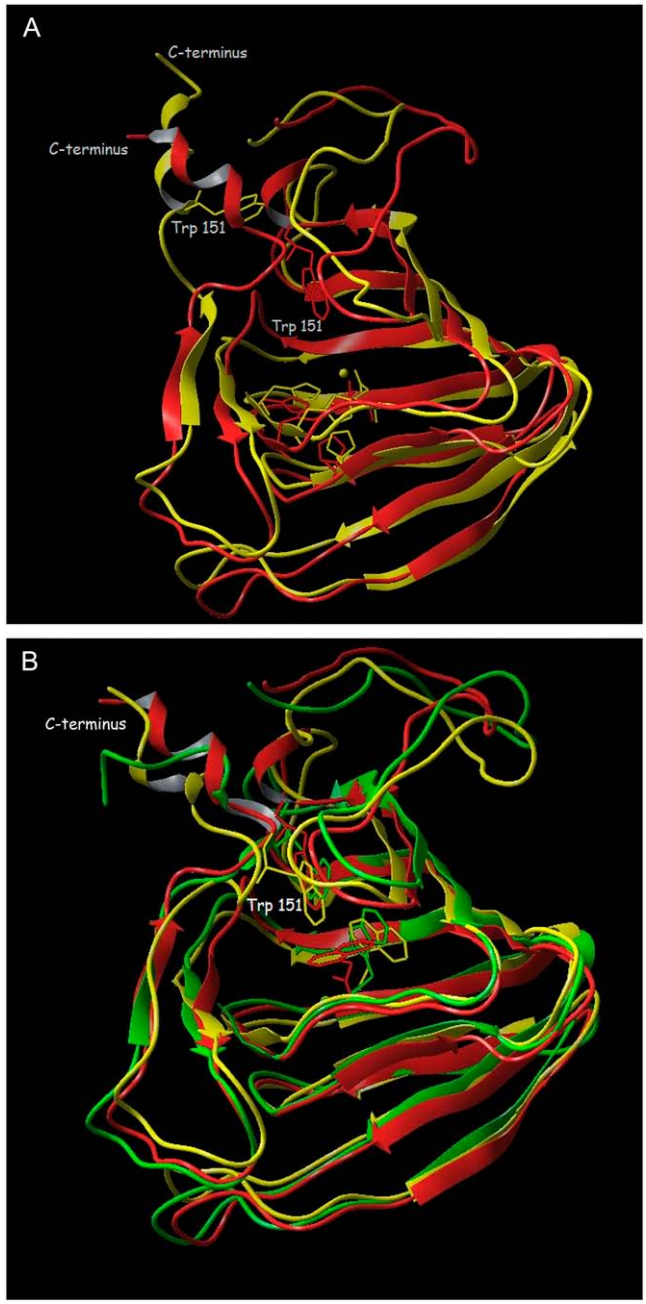

FIGURE 5 Superposition of the crystal structures and those obtained after 1.5 ns of simulation (at varying temperature). (*A*) The unbound ABP1, the crystal structure is colored red, and the simulated yellow. In the latter, the C-terminus is extended and tryptophan 151 is pulled out of the binding site (in which the zinc ion is shown as a sphere with its four coordinating residues). (*B*) The crystal structure of the ABP1-NAA complex (*red*) and the simulated structures of the ABP1-NAA complex (*yellow*) and the ABP1-IAA complex (*green*). Trp^{151}, Glu^{63}, and the ligand are shown in stick representation.

a structure with an extended C-terminus and tryptophan 151 outside the auxin binding site is an inactive conformation (with no auxin molecule bound). Similar results (the conformation with extended C-terminus being more stable) were obtained for the protein with the KDEL sequence added.

This conformational transition of the C-terminus is consistent with an earlier hypothesis (1,26,64) proposing a significant role for the C-terminus in the auxin signaling pathway.

Simulations performed for ABP1 complexes with NAA, IAA, and 3-IIBA revealed somewhat different dynamics of tryptophan 151 to that detected for the free ABP1. During the simulation period at 500 K, tryptophan 151 also moved away from the active site but, after cooling the system, it returned back into the active site (close to the aromatic ring of the ligand). The final structure was similar to the crystal structure, in particular with regard to the orientation and position of the C-terminus (Fig. 5 *B*). The only significant difference compared to the crystal structure was the position of the ligand, which was more buried inside the binding pocket but still close enough to tryptophan 151 to allow π-π interactions. From the results of the MD simulations, we conclude that the conformation found in the crystal structure of the ABP1-NAA complex is the active conformation stabilized by bound auxin. Comparison of the backbone RMSD to the crystal structure after 5 ns simulations at varying temperature revealed larger flexibility of the free ABP1 structure (RMSD = 3.51 Å) than of the ABP1-NAA complex (RMSD = 3.02 Å) (Fig. 6 *A*). The results of the MD simulations show that binding of an auxin molecule stabilizes the compact crystal structure and increases its population. This conformation is equivalent to the conformation found in the crystal structure of the ABP1-NAA complex and is probably the ABP1 active conformation as suggested by Woo et al. (26).

Both simulations at constant and at varying temperature detected the same hydrogen-bond network of water molecules. As expected (65), the exchange of water molecules is faster at higher temperature. During simulations at 300 K, water molecules entered and left the active site in 50 ps, while during simulations at varying temperature they exchanged within 10 ps. During simulations at 500 K, water molecules entered the zinc coordination sphere and changed the coordination of the auxin-related molecule from bidentate to monodentate. Such coordination was retained up to the end of the simulations (Fig. 6 *B*). More water molecules competed for the Zn coordination sphere until the drop of the temperature to 300 K. At room temperature, just one water molecule remained coordinated all the time.

To check the stability of the experimentally determined binding mode we manually docked NAA and 4-Cl-IAA in a few orientations that differ from the experimentally determined one and performed MD simulations. However, in all cases the auxin molecule reoriented back to the position found in the crystal structure.

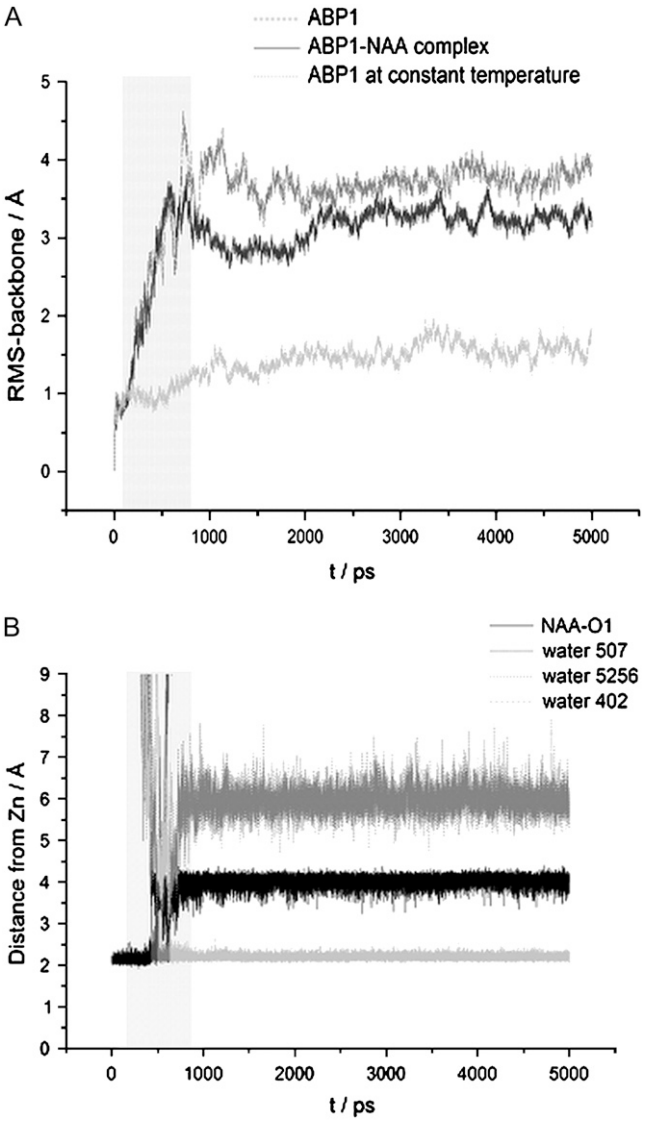

FIGURE 6 Analysis of the trajectories obtained during 5 ns of simulation with varying temperature. The period of simulations in which the temperature was maintained above 300 K is marked by the light gray box. (*A*) RMS deviations of the protein backbone from the corresponding crystal structure for the free ABP1 (*dark gray*) and the ABP1-NAA complex (*black*) in comparison with the RMSD for the free ABP1 simulated at a constant temperature (300 K) (*light gray*). (*B*) Distances between the zinc ion and the NAA oxygen atom (*black*), the oxygen atom of water molecules 1 (*dark gray*), 2 (*medium gray*), and 3 (*light gray*), during simulation of the ABP1-NAA complex.

RAMD simulations of auxin egress from the ABP1 binding site reveal three main routes: one to the membrane and two to the aqueous environment

Using the CAVER software (63), which is a geometrical tool for finding tunnels in a protein structure, three pathways were found (pwA, pwB, pwC, see below) from the active site to the protein exterior. These were later confirmed by RAMD simulations.

To simulate the egress of an auxin-related compound from the ABP1 binding pocket, we have run a number of random acceleration molecular dynamics (RAMD) simulations (52–54) using different magnitudes of random force applied to the substrate (see Methods). A smaller expelling force permits greater protein reorganization during the ligand egress

and gives more reliable results. At the same time, a smaller force implies longer simulations. To find the most suitable force magnitude, we performed 61 (34 with ABP1-NAA, 15 with ABP1-IAA, and 12 with ABP1-IIBA complexes) simulations changing the random force acceleration from 0.10 to 0.25 kcal/(g × Å) (Table 1). An acceleration of 0.20 kcal/(g × Å) proved to be most suitable. Auxin exit almost always occurred during 150 ps of simulation and a visual inspection indicated that the protein had enough time to accommodate to the changes in ligand position. Lower values of acceleration (0.10 and 0.15 kcal/(g × Å)) often did not result in auxin egress from the ABP1 binding site during 150 ps of simulation. With an acceleration of 0.25 kcal/(g × Å), the auxin molecule left the binding site too quickly, within 10 ps of simulations, and the protein structure did not have enough time to adjust to the auxin egress.

Different starting structures were used for the RAMD simulations. In some simulations, starting structures were equilibrated crystal structures of ABP1 with docked NAA or IAA. In other cases, structures obtained after 1.5 ns of simulation with variation in the temperature of the ABP1 complexes were used. Finally, we ran RAMD simulations using the structure with the extended C-terminus (obtained after 1.5 ns of simulation of ABP1 with temperature variation) with manually docked NAA, and the system equilibrated. Simulations of auxin egress did not reveal any large C-terminus

TABLE 1 Routes observed in the RAMD simulations

Starting structure	Acceleration (kcal/(g × Å))	Egress pathways	No. of trajectories*	Trajectory length (ps)	No. of trajectories with water entrance into the Zn-coordination†
ABP1 structure 1, NAA complex‡	0.10	—	1	150.0	—
	0.15	—	2	150.0	—
	0.20	—	2	150.0	—
	0.20	B	5	27.4–135.5	4
	0.20	A	1	63.5	0
	0.25	A	4	6.4–10.0	0
ABP1 structure 2, NAA complex§	0.10	—	2	150.0	—
	0.15	A	2	10.0	1
	0.20	A	2	6.0	1
ABP1 structure 1, IAA complex¶	0.15	—	1	150.0	—
	0.15	A	2	131.0–253.0	2
	0.17	A	2	17.5	2
	0.20	A_2	5	148.0	0
	0.20	A	2	11.5–12.0	1
	0.25	A_2	1	6.0	0
ABP1 structure 3, IAA complex‖	0.15	A	1	131.0	1
	0.20	A	1	11.5	1
ABP1 structure 4, NAA complex**	0.15	—	1	150.0	—
	0.15	B	3	95.0–182.5	2
	0.17	C	2	9.0–30.0	1
	0.20	A	1	6.0	1
	0.20	C	2	9.5	—
	0.20	B_2	2	8.5	1
	0.25	A	1	3.5	—
	0.25	B_2	1	4.5	1
ABP1 structure 1, IIBA complex††	0.13	—	1	250	—
	0.14	C	1	206	1
	0.15	C	2	68.5	2
	0.16	A	1	86.5	1
	0.17	C	3	16.5	3
	0.18	C	1	60.0	—
	0.20	C	3	16.5–151.5	3

*Several trajectories using different random number seeds for the random acceleration. Force directions were generated for each starting structure and random force acceleration magnitude.

†Number of trajectories during which, simultaneously with egress of carboxyl group from zinc coordination sphere, water molecule(s) enter into it.

‡Equilibrated structure of ABP1-NAA complex from crystal structure.

§Structure obtained after 1.5 ns of simulation of the ABP1-NAA complex with temperature variation.

¶Equilibrated structure of ABP1-IAA complex obtained from ABP1 crystal structure with IAA manually docked into the binding site.

‖Structure obtained after 1.5 ns of simulation of the ABP1-IAA complex with temperature variation.

**Structure obtained after 1.5 ns of simulation of the free ABP1 in which NAA was manually docked for RAMD simulations.

††Equilibrated structure of ABP1-IIBA complex obtained from ABP1 crystal structure with IIBA manually docked into the binding site.

movement. During some RAMD simulations, the entrance of water molecules into the zinc coordination sphere occurred simultaneously with an auxin expulsion (Table 1). This finding indicates the possible role of water molecules in helping the auxin molecule to leave the zinc coordination sphere in ABP1.

Using RAMD simulations of the ABP1-NAA complex, three main egress routes were identified. Pathway A (pwA) leads through the protein loop closed by prolines 126 and 127 on one side, and alanine 33 on the other side (Fig. 7). Route B (pwB) leads through the center of the protein surrounded by β-sheets (Fig. 7) and ends at the hole on the protein surface surrounded by phenylalanines 92, 93, and 98, and threonine 96. Pathway C (pwC) leads from the active site through two loops, in the vicinity of proline 148 and phenylalanine 149 at one, and of glutamine 17 and glycine 21 at the other side (Fig. 7). Besides these three main routes, in some simulations one of two other pathways was observed, pwA_2 and pwB_2. Routes pwA_2 and pwB_2 are practically the same as routes pwA and pwB, respectively. In both cases, differences in the auxin egress are probably due to differences in the starting structures used in the RAMD simulations. As the protein loop which contains prolines 126 and 127 is flexible, the auxin exits either below it (pwA_2), or above it (pwA) (Fig. 7). A similar difference is observed between pwB_2 and pwB (Fig. 7).

In 52 simulations that resulted with ligand egress from active site of ABP1, pwA was used 26 times and pwB 11 and pwC 14 times. It is important to stress that pwC was mostly used by antiauxin molecule (10 out of the 14 simulations that ended with pwC egress were simulations of IIBA egress from ABP1 binding site).

In nine out of 11 simulations in which the ligand molecule used pwB, a water molecule entered the zinc coordination sphere. For route pwA, this happened in 10 out of 25 times and for route pwC in 10 out of 14 times. The entrance of a water molecule into the coordination sphere of zinc during auxin exit suggests that one of the roles of water molecules in the active site is to help auxin to leave the zinc coordination sphere. The route by which water enters the ABP1 binding site is close to pwA, but it is a distinct channel.

If the orientation of ABP1 with respect to the membrane proposed by Woo et al. is correct (Fig. 7), the three main pathways have different functions. Pathway A would lead from the ABP1 active site to the membrane, while pathways B and C would lead from the binding site to the lumen of the ER, cytosol, or apoplast, depending on the ABP1 location. In any case, pwA would be the route used by auxin to travel between the membrane and the ABP1 binding site, while pwB and pwC would be the pathways for auxin to travel between the binding site and the ABP1 surroundings.

The arrangement of the ABP1 monomers in the homodimer as determined in the crystal structures is such that it does not obstruct movement of auxin molecules through the pathways found. Pathways A and A_2 connect the ABP1 binding site to the membrane and pathways B, B_2, and C connect it to the ABP1 surroundings (Fig. 8).

Mechanistic and biological implications of the molecular modeling results

The results of the MD simulations of the ABP1 and its complexes with different auxin-related compounds reveal some important characteristics of this protein and allow us to propose a binding mechanism. ABP1 is a quite rigid protein (26) that keeps its firm β-skeleton structure during all MD simulations, at room and at elevated (500 K) temperatures. The only part of the structure that changed significantly during the simulations, and then only at elevated temperatures (500 K), was the C-terminus that extended and pulled

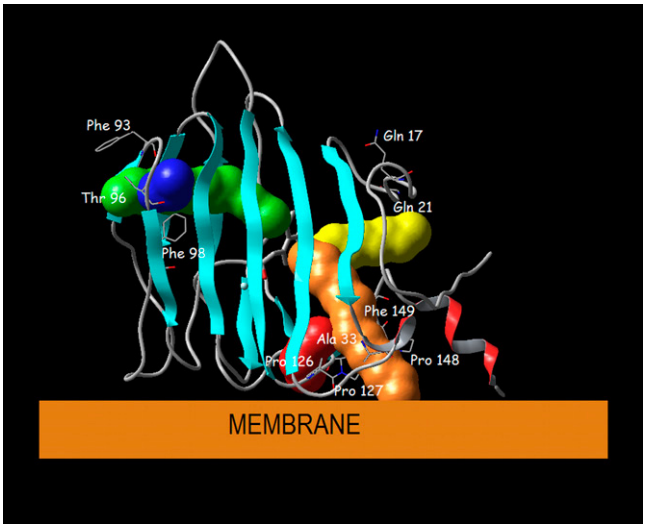

FIGURE 7 Orientation of ABP1 toward the membrane proposed by Woo et al. with possible auxin egress pathways displayed: the main (most frequently found) routes are pwA (*orange*), pwB (*green*), and pwC (*yellow*), and the rarely found routes are pwA_2 (*red*) pwB_2 (*blue*).

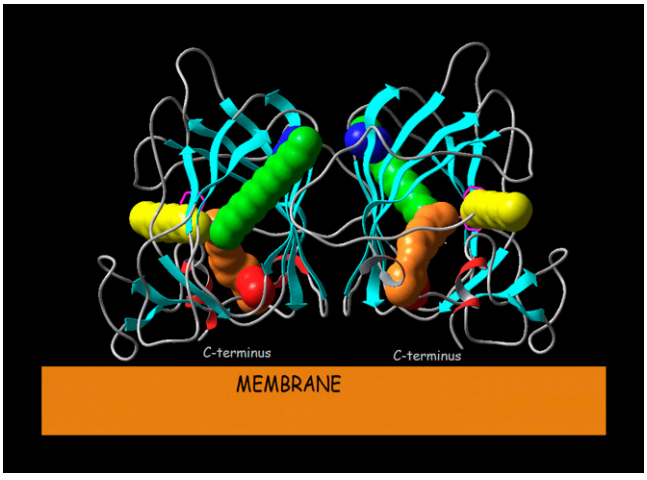

FIGURE 8 Orientation of the ABP1 homodimer to the membrane with possible pathways for auxin entrance/exit from the binding sites shown for pwA ((*orange*), pwB (*green*), pwA_2 (*red*), pwB_2 (*blue*), and pwC (*yellow*)).

tryptophan 151 out of the binding pocket. This occurred only during the simulations of the free ABP1, whereas in the complex with an auxin molecule, tryptophan 151 remained in the binding site and participated in π-π interactions with the ligand (Fig. 5). Apparently, the auxin molecule stabilizes the protein structure and makes it more rigid (Fig. 6 *A*). Our observation that binding of an auxin molecule influences only the flexibility and location of the α-helical C-terminus, but does not effect the structure of the ABP1 β-barrel is consistent with the hypothesis that the movement of the C-terminus might be the first step, after auxin binding, in the auxin signaling pathway. The importance of the ABP1 C-terminus is shown by experimental findings that the presence of a synthetic peptide corresponding to the C-terminus can activate auxin response and induces hyperpolarization of the membrane (34,66) and protoplast swelling (67). Further, experiments on ABP1 protein and its mutants showed that the KDEL sequence is not essential for ABP1 activity, including auxin binding and interaction with the plasma membrane (68). Our hypothesis is that, in the plant cell, the free ABP1 (without an auxin bound) has predominantly the conformation with the C-terminus extended. Binding of an auxin molecule stabilizes a conformation with tryptophan 151 in the active site and with a less extended C-terminus (similar to the one found in the crystal structure (Fig. 5)), and it becomes the most populated. The shift in equilibrium population of conformations toward more rigid ones is probably connected with the signal transfer. Changes in the ABP1 conformations caused by auxin binding have been experimentally shown by an immunological approach (35). This supports the hypothesis that ABP1 is indeed an auxin receptor, i.e., it mediates the faster responses to auxin presence in the plant cell (6,24).

Simulations of auxin egress from ABP1 revealed three main routes for auxin-related molecules to enter and leave the active site. With the proposed orientation(s) of ABP1 toward the membrane (26) (Fig. 7), pwA would be the route for auxin travel between the membrane and the ABP1 active site while pwB and pwC would be the routes that would enable auxin to travel between the active site and the ABP1 surroundings. As the outer side of the plasma membrane is the most probable location at which ABP1 acts as an auxin receptor, we propose that pwB or pwC is used by an auxin molecule to enter into the binding site and pwA to exit into the membrane after it has stabilized the conformation with a less extended C-terminus (the active conformation). This finding is confirmed by RAMD simulations of auxin egress from the inactive conformation, i.e., the conformation with an extended C-terminus and tryptophan 151 pulled out of the active site (Table 1) where pwB and pwC were predominantly observed (in 10 out of 12 simulations). The fact that the antiauxin compound (IIBA) used mostly pwC during simulations gives a possible explanation for its inhibitory behavior: IIBA can easily enter the ABP1 binding site but has more difficulty leaving it and because of this, it inhibits auxin activity.

A significant finding, consistently observed in all simulations, is the movement of water molecules from the bulk solvent into the active site. Water molecules always entered through the same channel generating a network of hydrogen-bonded water molecules from the protein surface to the active site. In all simulations at constant temperature (300 K), the water molecule closest to the binding site is hydrogen-bonded to the carboxylate groups of glutamate 63 and the auxin simultaneously. Both these negatively charged carboxylate groups come close to each other when coordinated to the zinc ion. A possible role of the water molecule is to reduce their repulsion by acting as a proton donor in hydrogen bonds (Fig. 4). During simulations at elevated temperature, a water molecule entered into the coordination sphere of the zinc and replaced the oxygen of the carboxyl group of auxin which became a monodentate ligand. In RAMD simulations, the auxin expulsion was accompanied by the return of water to the zinc coordination. It can be assumed that water molecules in the ABP1 active site assist the release of auxin from the zinc coordination sphere. A possible role of water molecules in the ABP1 mechanism might also be to regulate protonation and deprotonation of the auxin-related compound. It is most likely that an auxin-related compound coordinates zinc with a deprotonated carboxyl group, but passes the membrane as a neutral species. Therefore, ABP1 should have a mechanism enabling protonation and deprotonation of an auxin-related compound. The hydrogen-bond network of water molecules spanning from the active site to the protein surface could provide the means for transferring a proton to or from the auxin carboxyl group.

CONCLUSIONS

Molecular modeling and simulation were applied to study auxin binding to the ABP1 to shed light on the physiological role of ABP1. Using molecular dynamics simulations, two different conformations of ABP1 were found. The conformation of ABP1 with the extended C-terminus and tryptophan 151 pulled out from binding site may be adopted when no auxin-related molecule is bound. Binding of an auxin-related compound stabilizes the other, more rigid conformation, in which tryptophan 151 is engaged in π-π interactions with the planar aromatic group of the auxin-related compound, and the C-terminus is not extended. The observed influence of auxin binding on the structure and flexibility of the C-terminus is in accord with experiments that have revealed its role in the auxin-induced changes of the plasma membrane.

The observed hydrogen-bond network of water molecules between the ABP1 binding site and the protein surface indicates potential roles for water in the ABP1-auxin binding mechanism. One is to facilitate auxin unbinding by a water molecule replacing the auxin in the zinc coordination sphere, and the other is to guide the proton transfer through the hydrogen-bonded water network during the protonation/deprotonation of the auxin compound.

RAMD simulations showed three pathways which an auxin-related compound can use to enter and leave the ABP1 binding site. As the pathways connect the active site of ABP1 and different sides of the protein surface, and the frequency of their appearance is related to the protein conformation, we suggest that pwB and pwC are used by the ligand to enter and pwA to leave the ABP1 active site. If the proposed orientation of the ABP1 to the membrane (26) is correct, pwA leads to the membrane and pwB and pwC lead to ABP1's aqueous surroundings.

We are grateful to Dr. Darko Babić (Ruđer Bošković Institute) for his help in installing the programs on the computer cluster and running the calculations on it. We thank Tim Johann (EML Research) for the help that he provided us with installation of the tools for RAMD simulations. We are also grateful to the ''SRCE'' computing center in Zagreb whose computer cluster was used for most of the calculations. Our thanks go to Prof. Dr. Richard Napier (Warwick HRI, University of Warwick, Warwick, UK) for valuable discussion and to Dr. Vlad Cojocaru (EML Research) for critical reading of the manuscript.

We gratefully acknowledge support from the German-Croatian Bilateral Cooperation grant (No. WTZ-HRV01/010) and the Klaus Tschira Foundation.

REFERENCES

1. Davies, P. J. 2004. Plant Hormones: Biosynthesis, Signal Transduction, Action. Kluwer Academic Publishers, Dordrecht, Netherlands.
2. Perrot-Rechenmann, C., and R. M. Napier. 2005. Auxins. *Vitam. Horm.* 72:203–233.
3. Napier, R. M., K. M. David, and C. Perrot-Rechenmann. 2002. A short history of auxin-binding proteins. *Plant Mol. Biol.* 49:339–348.
4. Woodward, A. W., and B. Bartel. 2005. Auxin: regulation, action, and interaction. *Ann. Bot.* (*Lond.*). 95:707–735.
5. Kepinsky, F., and O. Leyser. 2005. Plant development: auxin in loops. *Curr. Biol.* 15:208–210.
6. Teale, W. D., I. A. Paponov, and K. Palme. 2006. Auxin in action: signaling, transport and the control of plant growth and development. *Nat. Rev. Mol. Cell Biol.* 7:847–859.
7. Thimann, K. V. 1977. Hormone Action in the Whole Life of Plants. The University of Massachusetts Press, Amherst, MA.
8. Lüthen, H., M. Claussen, and M. Böttger. 1999. Growth: progress in auxin research. *Prog. Bot.* 60:315–340.
9. Weijers, D., and G. Jürgens. 2004. Funneling auxin action: specificity in signal transduction. *Curr. Opin. Plant Biol.* 7:687–693.
10. Friml, J. 2003. Auxin transport-shaping the plant. *Curr. Opin. Plant Biol.* 6:7–12.
11. Jones, A. M. 1998. Auxin transport: down and out and up again. *Science.* 282:2201–2202.
12. Scheres, B., and J. Xu. 2006. Polar auxin transport and patterning: growth with the flow. *Genes Dev.* 20:922–926.
13. Ciesielski, T. 1872. Downward curvature of the root. *Beitrage zur Biologie der Pflanzen.* 1:1–30.
14. Darwin, C. 1880. The Power of Movement in Plants. J. Murray, London, UK.
15. Went, F. W. 1927. On growth accelerating substances in the coleoptile of *Avena sativa. Proc. Kon. Ned. Akad. Wet.* 30:1–19.
16. Went, F. W. 1928. The growth substance and growth. *Rev. Trav. Bot. Neerl.* 25:1–116.
17. Kögel, F., and D. G. F. R. Kostermans. 1934. Heteroauxin as a metabolite of lower plant-like organisms. Isolation from yeast. *Hoppe-Seyler's Z. Physiol. Chem.* 228:113–121.
18. Thiman, K. V. 1935. On the plant growth hormone produced by *Rhizopus suinus. J. Biol. Chem.* 109:279–291.
19. Petrásek, J., J. Mravec, R. Bouchard, J. J. Blakeslee, M. Abas, D. Seifertová, J. Wisniewska, Z. Tadele, M. Kubes, M. Covanová, P. Dhonukshe, P. Skupa, E. Benková, L. Perry, P. Krecek, O. R. Lee, G. R. Fink, M. Geisler, A. S. Murphy, C. Luschnig, E. Zazímalová, and J. Friml. 2006. PIN proteins perform a rate-limiting function in cellular auxin efflux. *Science.* 312:914–918.
20. Wiśniewska, J., J. Xu, D. Seifertová, P. B. Brewer, K. Rũžička, I. Blilou, D. Rouquié, E. Benková, B. Scheres, and J. Friml. 2006. Polar PIN localization directs auxin flow in plants. *Science.* 312:883–885.
21. Dharmasiri, S., R. Swarup, K. Mockaitis, N. Dharmasiri, S. K. Singh, M. Kowalchyk, A. Marchant, S. Mills, G. Sandberg, M. J. Bennett, and M. Estelle. 2006. AXR4 Is required for localization of the auxin influx facilitator AUX1. *Science.* 312:1218–1220.
22. Siberer, T., and O. Leyser. 2006. Auxin transport, but in which direction? *Science.* 312:858–860.
23. Paciorek, T., and J. Friml. 2006. Auxin signaling. *J. Cell Sci.* 119: 1199–1202.
24. Badescu, G. O., and R. M. Napier. 2006. Receptors for auxin: will it all end in TIRs? *Trends Plant Sci.* 11:217–223.
25. Woodward, A. W., and B. Bartel. 2005. A receptor for auxin. *Plant Cell.* 17:2425–2429.
26. Woo, E.-J., J. Marshall, J. Bauly, J.-G. Chen, M. Venis, R. M. Napier, and R. W. Pickersgill. 2002. Crystal structure of auxin-binding protein 1 in complex with auxin. *EMBO J.* 21:2877–2885.
27. Dharmasiri, N., S. Dharmasiri, and M. Estelle. 2005. The F-box protein TIR1 is an auxin receptor. *Nature.* 435:441–445.
28. Kepinski, S., and O. Leyser. 2005. The *Arabidopsis* F-box protein TIR1 is an auxin receptor. *Nature.* 435:446–451.
29. Gray, W. M., S. Kepinski, D. Rouse, O. Leyser, and M. Estelle. 2001. Auxin regulates $SCFP^{TIR1P}$-dependent degradation of AUX/IAA proteins. *Nature.* 414:271–276.
30. Napier, R. M. 2001. Models of auxin binding. *J. Plant Growth Regul.* 20:244–254.
31. Klämbt, D. 1990. A view about the function of auxin binding proteins at plasma membranes. *Plant Mol. Biol.* 14:1045–1050.
32. Feldwisch, J., R. Zettl, F. Hesse, J. Schell, and K. Palme. 1992. An auxin binding protein is located to the plasma membrane of maize coleoptile cells: identification by photoaffinity labeling and purification of a 23-kDa polypeptide. *Proc. Natl. Acad. Sci. USA.* 89:475–479.
33. Jones, A. M., and M. A. Venis. 1989. Photoaffinity labeling on auxin-binding protein in maize. *Proc. Natl. Acad. Sci. USA.* 86:6153–6156.
34. Leblanc, N., C. Perrot-Rechenmann, and H. Barbier-Brygoo. 1999. The auxin-binding protein Nt-ERabp1 alone activates an auxin-like transduction pathway. *FEBS Lett.* 449:57–60.
35. Leblanc, N., K. David, J. Grosclaude, J.-M. Pradier, H. Barbier-Brygoo, S. Labiau, and C. Perrot-Rechenmann. 1999. A novel immunological approach establishes that the auxin-binding protein, Nt-abp1, is an element involved in auxin signaling at the plasma membrane. *J. Biol. Chem.* 274:28314–28320.
36. Campanoni, P., and P. Nick. 2005. Auxin-dependent cell division and cell elongation. 1-Naphthaleneacetic acid and 2,4-dichlorophenoxyacetic acid activate different pathways. *Plant Phys.* 137:939–948.
37. Löbler, M., and D. Klämbt. 1985. Auxin-binding protein from coleoptile membranes of corn (*Zea mays* L.). *J. Biol. Chem.* 260:9848–9853.
38. Inohara, S., S. Shimomura, T. Fukui, and M. Futai. 1989. Auxin-binding protein located in the endoplasmic reticulum of maize shoots: molecular cloning and complete primary structure. *Proc. Natl. Acad. Sci. USA.* 86:3564–3568.
39. Hesse, T., J. Feldwisch, D. Balshüsemann, G. Bauw, M. Puype, J. Vandekerckhove, M. Löbler, D. Klämbt, J. Schell, and K. Palme. 1989. Molecular cloning and structural analysis of a gene from *Zea mays* (L.) coding for a putative receptor for the plant hormone auxin. *EMBO J.* 8:2453–2461.

40. Henderson, J., J. M. Bauly, D. A. Ashford, S. C. Oliver, C. R. Hawes, C. M. Lazarus, M. A. Venis, and R. M. Napier. 1997. Retention of maize auxin-binding protein in endoplasmic reticulum: quantifying escape and the role of auxin. *Planta*. 202:313–323.

41. Dunwell, J. M., A. Purvis, and S. Khuri. 2004. Cupins: the most functionally diverse protein superfamily? *Phytochemistry*. 65:7–17.

42. Woo, E. J., J. M. Dunwell, P. Goodenough, A. C. Marvier, and R. W. Pickersgill. 2000. Germin is a manganese containing homohexamer with germin and superoxide dismutase activities. *Nat. Struct. Biol.* 7:1036–1040.

43. Bertoša, B., B. Kojić-Prodić, R. C. Wade, M. Ramek, S. Piperaki, A. Tsantili-Kakoulidou, and S. Tomić. 2003. A new approach to predict the biological activity of molecules based on similarity of their interaction fields and the log*P* and log*D* values: application on auxines. *J. Chem. Inf. Comput. Sci*. 43:1532–1541.

44. Tomić, S., R. R. Gabdouline, B. Kojić-Prodić, and R. C. Wade. 1998. Classification of auxine plant hormones by interaction property similarity indices. *J. Comput. Aided Mol. Des.* 12:63–79.

45. Porter, W. L., and K. V. Thimann. 1965. Molecular requirements for auxin action. *Phytochemistry*. 4:229–243.

46. Katekar, G. F. 1979. Auxins: on the nature of the receptor site and molecular requirements for auxin activity. *Phytochemistry*. 18:223–233.

47. Farrimond, J. A., M. C. Elliott, and D. W. Clark. 1978. Charge separation as a component of the structural requirements for hormone activity. *Nature*. 274:401–402.

48. Kaethner, T. M. 1977. Conformational change theory for auxin structure-activity relationship. *Nature*. 267:19–23.

49. Edgerton, M. D., A. Tropsha, and A. M. Jones. 1994. Modeling the auxin-binding site of auxin-binding protein 1 of maize. *Phytochemistry*. 35:1111–1123.

50. Rescher, U., A. Walther, C. Schiebl, and D. Klambt. 1996. In vitro I binding affinities of 4-chloro-, 2-methyl-, 4-methil-, and 4-ethylindolacetic acid to auxin-binding protein 1 (ABP1) correlate with their growth-stimulating activities. *J. Plant Growth Regul*. 15:1–3.

51. Ray, P. M. 1977. Specificity of auxin-binding sites on maize coleoptile membranes as possible receptor sites for auxin action. *Plant Physiol*. 60:585–591.

52. Schleinkofer, K., P. J. Sudarko, R. C. Winn, S. K. Lüdemann, and R. C. Wade. 2005. Do mammalian cytochrome P450a show multiple ligand access pathways and ligand channeling? *EMBO Rep*. 6:584–589.

53. Lüdemann, S. K., V. Lounnas, and R. C. Wade. 2000. How do substrates enter and products exit the buried active site of cytochrome P450cam? 2. Steered molecular dynamics and adiabatic mapping of substrate pathways. *J. Mol. Biol*. 303:813–830.

54. Winn, P. J., S. K. Lüdemann, R. Gauges, V. Lounnas, and R. C. Wade. 2002. Comparison of the dynamics of substrate access channels in the three cytochrome P450s reveals different opening mechanisms and a novel functional role for buried arginine. *Proc. Natl. Acad. Sci. USA*. 99:5361–5366.

55. Berman, H. M., J. Westbrook, Z. Feng, G. Gilliland, T. N. Bhat, H. Weissig, I. N. Shindyalov, and P. E. Bourne. 2000. The Protein Data Bank. *Nucleic Acids Res*. 28:235–242.

56. Case, D. A., T. A. Darden, T. E. Cheatham III, C. L. Simmerling, J. Wang, R. E. Duke, R. Luo, K. M. Merz, B. Wang, D. A. Pearlman, M. Crowley, S. Brozelli, V. Tsui, H. Gohlke, J. Mongan, V. Hornak, G. Cui, P. Beroza, C. Schafmeister, J. W. Caldwell, W. S. Ross, and P.A. Kollman. 2004. AMBER 8, University of California, San Francisco.

57. Pearlman, D. A., D. A. Case, J. W. Caldwell, W. S. Ross, T. E. Cheatham III, S. DeBolt, D. Ferguson, G. Seibel, and P. Kollman. 1995. AMBER, a package of computer programs for applying molecular mechanics, normal mode analysis, molecular dynamics and free energy calculations to simulate the structural and energetic properties of molecules. *Comput. Phys. Commun*. 91:1–41.

58. Tomić, S., L. Nilsson, and R. C. Wade. 2000. Nuclear receptor-DNA binding specificity: a combine and free-Wilson QSAR analysis. *J. Med. Chem.* 43:1780–1792.

59. Vriend, G. 1990. WHAT IF: a molecular modeling and drug design program. *J. Mol. Graph.* 8:52–56.

60. Duan, Y., C. Wu, S. Chowdhury, M. C. Lee, G. Xiong, W. Zhang, R. Yang, P. Cipelak, R. Luo, and T. Lee. 2003. A point-charge force field for molecular mechanics simulations of proteins. *J. Comput. Chem.* 24:1999–2012.

61. Callahan, T. J., E. Swanson, and T. P. Lybrand. 1996. MD Display: an interactive graphics program for visualization of molecular dynamics trajectories. *J. Mol. Graph.* 14:39–41.

62. Pettersen, E. F., T. D. Goddard, C. C. Huang, G. S. Couch, D. M. Greenblatt, E. C. Meng, and T. E. Ferrin. 2004. UCSF Chimera—a visualization system for exploratory research and analysis. *J. Comput. Chem.* 25:1605–1612.

63. Petrek, M., M. Otyepka, P. Banas, P. Kosinova, J. Koca, and J. Damborsky. 2006. CAVER: a new tool to explore routes from protein clefts, pockets and cavities. *BMC Bioinformatics*. 7:316–325.

64. Warwicker, J. 2001. Modeling of auxin-binding protein 1 suggest that its C-terminus and auxin could compete for a binding site that incorporates a metal ion and tryptophan residue 44. *Planta*. 212:343–347.

65. Garcia, A. E., and G. Hummer. 2000. Water penetration and escape in proteins. *PROTEINS Struct. Funct. Gen.* 38:261–272.

66. Thiel, G., M. R. Blatt, M. D. Fricker, I. R. White, and P. Milllner. 1993. Modulation of KP^{+P} channels in *Vicia* stomatal guard cells by peptide homologs to the auxin-binding protein C-terminus. *Proc. Natl. Acad. Sci. USA*. 90:11493–11497.

67. Steffens, B., C. Feckler, K. Palme, M. Christian, M. Bottger, and H. Luthen. 2001. The auxin signal for proptoplast swelling is perceived by extracellular ABP1. *Plant J*. 27:591–599.

68. David, K., E. Carnero-Diaz, N. Leblanc, M. Monestiez, J. Grosclaude, and C. Perrot-Rechenmann. 2001. Conformational dynamics underlie the activity of auxin-binding protein, Nt-abp1. *J. Biol. Chem.* 276:34517–34523.